Food Control 188 (2026) 112219

Contents lists available at ScienceDirect

Food Control

journal homepage: www.elsevier.com/locate/foodcont

# Active bio-based packaging for fresh-cut melon: Antimicrobial efficacy and zinc migration of nanocellulose/ZnO nanocomposite films

Ana Rita Mendes [a], Francisco A.G. Soares Silva [a], Cristina Mena [b], Fátima Silva [b], Cristina L.M. Silva [a], Paula Teixeira [a], Fátima Poças [a,b,*]

[a] Universidade Católica Portuguesa, CBQF - Centro de Biotecnologia e Química Fina – Laboratório Associado, Escola Superior de Biotecnologia, Rua Diogo Botelho 1327, 4169-005, Porto, Portugal

[b] CINATE, Escola Superior de Biotecnologia, Universidade Católica Portuguesa, Rua Diogo Botelho 1327, 4169-005, Porto, Portugal

ARTICLE INFO

*Keywords:*
Zinc oxide nanoparticles
Active food packaging
Shelf life extension
Fresh-cut melon
Zinc migration
Nanocellulose films
Bio-based materials

ABSTRACT

Growing environmental concerns, together with the need to extend shelf life and protect food from pathogens and mechanical damage, are driving the development of innovative active packaging materials. In this study, nanocellulose (NC) films incorporating zinc oxide nanoparticles (ZnO NPs) with three different morphologies (spherical, sheet and flower) were produced by solvent casting for food packaging applications. Films were characterised by scanning electron microscopy (SEM), and antimicrobial activity was addressed by agar diffusion assay against *Escherichia coli* and *Staphylococcus aureus*. NC/ZnO films were used as package for fresh-cut melon, which was stored at 4 °C for one week, and subjected to microbiological, pH and zinc migration analysis.

SEM revealed a porous, and nanofibrillar cellulose, suitable for nanoparticles (NPs) retention, while cross sections showed the dispersion of NPs among the films. *In vitro* antimicrobial studies demonstrated the influence of morphology, with the sheet shape producing the highest inhibitory halos. In contact with melon, NC/ZnO films suppressed microbial proliferation relative to controls, keeping microbiological levels within acceptable limits up to day 7. Sheet shape showed the most significant effect. Total Zn migration plateaued at 7–8 mg $kg^{-1}$ under a realistic area-to-mass scenario, with no significant differences among morphologies. Measurements reflect total Zn after acid digestion and ionic versus particulate species could not be distinguished. NC/ZnO films maintained slightly higher pH than controls.

Overall, these findings highlight the potential of bio-based NC/ZnO films to extend melon shelf life, with antimicrobial efficacy strongly influenced by nanoparticle morphology.

## 1. Introduction

Consumers are increasingly interested in minimally processed foods due to their health benefits. Fresh fruits and vegetables are a priority in many purchasing decisions, as they provide vitamins, minerals, dietary fibre, and antioxidants that support a balanced diet (Török et al., 2023). However, these foods are unstable after harvesting due to physical damage, biochemical changes, moisture loss, microbial proliferation, and oxidative deterioration, compromising quality and shelf life (Venkatesan & Muniyan, 2024). Packaging plays an important role in preserving product quality during storage, handling, and final use. In particular, active packaging has gained significant attention for its ability to extend shelf life, preserve freshness, and enhance safety by limiting the growth of potentially hazardous bacteria (Ahmed et al., 2022; Fadiji et al., 2023; Pascall, 2020). Additionally, by reducing spoilage, active packaging can also help in decreasing food waste and lowering corresponding environmental impacts. Growing global concern about sustainability is driving the replacement of petroleum-based plastics with bio-based, environmentally friendly materials (Basumatary et al., 2022; Dejene et al., 2024).

Within this context, nanocellulose (NC) is a natural polymer derived from various plants and agricultural products, increasingly used for paper and paperboard, biomedical products, food packaging, and textiles (Zhang et al., 2023). Nanofibrillated cellulose comprises long, flexible fibrils with at least one dimension in the nanometre range, containing abundant hydroxyl groups that enable surface modifications

* Corresponding author. Universidade Católica Portuguesa, CBQF - Centro de Biotecnologia e Química Fina – Laboratório Associado, Escola Superior de Biotecnologia, Rua Diogo Botelho 1327, 4169-005, Porto, Portugal.

*E-mail addresses:* s-anrimamendes@ucp.pt (A.R. Mendes), fpocas@ucp.pt (F. Poças).

https://doi.org/10.1016/j.foodcont.2026.112219
Received 29 January 2026; Received in revised form 28 March 2026; Accepted 14 April 2026
Available online 15 April 2026

and strong bonding networks (Hansini et al., 2025; Soares Silva et al., 2020). The resulting porous matrix is an effective carrier for active compounds as it stabilises inorganic fillers and metal ions via hydrogen bonding through electrostatic interactions (Kumar et al., 2025; Roy et al., 2021). For food contact applications, cellulose is also used as reinforcing agent to improve physicochemical and functional properties (Maloufi et al., 2025; Singh et al., 2025).

Zinc oxide nanoparticles (ZnO NPs) stand out for their broad-spectrum of antimicrobial activity, UV blocking capability, and high surface-to-volume ratio, and are therefore of interest to be incorporated into bio-based polymers for food contact materials (FCM) (Lebaka et al., 2025; Dejene and Abtew, 2025). Antimicrobial efficacy is strongly dependent on particle size and morphology, which modulate the reactive oxygen species (ROS) generation and $Zn^{2+}$ release. Together, these pathways disrupt bacterial cells, inhibiting their proliferation (Kim et al., 2022; Mendes et al., 2025). Despite these functional advantages, potential Zn migration raises concerns about toxicological risk against human health and regulatory compliance. Presently, ZnO (nano) is considered safe by the European Food Safety Authority (EFSA), as an ultraviolet light absorber for plastic FCM (EFSA, 2016). Although extensive literature has documented the antimicrobial role of ZnO and its migration into food simulants (Bumbudsanpharoke et al., 2019; Peter et al., 2022; Singh et al., 2024), studies addressing migration into real food models are scarce. Most available data relate to meat products, particularly poultry (Sasidharan et al., 2024; Soares Silva et al., 2023; Souza et al., 2020).

To address this gap, melon fruit was selected for shelf life studies because it has high water activity, which promotes rapid microbial growth even under refrigeration. In addition, melon is commonly commercialized and highly appreciated by consumers in a ready-to-eat cube format, which increases its exposed surface area and, consequently, accelerates microbial spoilage. Therefore, developing a packaging system that enables the assessment of antimicrobial efficacy and zinc migration is particularly relevant. Most previous studies on active packaging for melon have focused on chitosan- or alginate-based films incorporated with silver nanoparticles (NPs), mainly assessing quality attributes, microbial safety, and sensory evaluation (Danza et al., 2015; Ortiz-Duarte et al., 2019; Sun et al., 2022). Only one study has tested cellulose absorbent pads containing silver NPs (Fernández et al., 2010), and studies using ZnO NPs or investigating nanoparticle migration into melon are absent, underscoring the novelty of the present work. In fact, ZnO NPs offer advantages over silver, as they combine lower toxicity and lower production cost with a more sustainable production process (Karuppan Perumal et al., 2025).

Regarding the legislative framework, Regulation (EU) No. 2073/2005 lays down microbiological criteria for foodstuffs, providing a well-established control standard for microbial hazards (European Commission, 2005). In contrast, there is a concern and regulatory gap regarding safety of NPs if their migration occurs. According to Regulation (EU) No. 1935/2004, FCM must not release their constituents into food in quantities that could compromise human health, cause unacceptable changes in the food's composition, or deteriorate its organoleptic characteristics (European Commission, 2004). For plastic materials, Regulation (EU) No. 10/2011 sets a specific migration limit (SML) for ionic zinc of 5 mg $kg^{-1}$ of food, while indicating that nanoparticles require a case-by-case risk assessment (European Commission, 2011). Additionally, EFSA reported that ZnO NPs do not migrate in nanoparticulate form when incorporated in an unplasticized polymer, so safety assessment should focus on soluble ionic zinc ($Zn^{2+}$) (EFSA, 2016). However, these assessments were performed only for plastic materials, where the NPs are strongly embedded in the polymeric matrix. In more porous systems, such as cellulose-based materials (ex, films or absorption pads), different migration profiles can occur, requiring case-by-case risk assessment. In fact, a previous study concluded that both ionic Zn and nanoparticle ZnO migrated from nanocellulose films into food simulants (Mendes et al., 2026). Therefore, additional research using real food models is needed to address this regulatory gap and complement the existing regulatory framework (Poças & Franz, 2018).

In this context, the present work aims to develop NC nanocomposites incorporating ZnO NPs with three morphologies (spherical, sheet, and flower) and evaluate their performance in a fresh-cut melon model. The films were first characterised regarding their structure and nanoparticle distribution, and agar diffusion assays were performed to confirm *in vitro* antimicrobial efficacy. The films were then applied to melon slices and stored under refrigeration over one week. Microbiological counts and pH were monitored for shelf life assessment. Total Zn migration over time was quantified by atomic absorption spectrometry (AAS) after acid digestion, providing a realistic exposure scenario in a real-food matrix. By combining microbial shelf life studies with migration analysis, this study provides new data on the safety and functionality of bio-based NC/ZnO nanocomposite packaging. The results are expected to contribute to the current knowledge gap between studies using food simulants and those in real food systems, and to support regulatory assessment of nanomaterials in food contact applications.

## 2. Materials and methods

### 2.1. Preparation of NC/ZnO NPs nanocomposite films

The ZnO NPs employed in this work were synthesized via sol-gel method in three different morphologies: spherical (ZnO-SP), flower (ZnO-FL), and sheet shape (ZnO-SH), represented in Fig. S1. Their physicochemical and functional properties have already been extensively characterized in earlier studies, and a summary of these data is provided in Table S1 (Mendes et al., 2024, 2025).

NC/ZnO composite films were obtained through the solvent casting technique. The nanocellulose Valida S231C 3% (Sappi Biochemtech BV, Maastricht, Netherlands) was used. This material originates from wood pulp and presents fibrils with widths between 20 and 60 nm and lengths distribution mainly below 31 μm, as reported by the supplier's technical datasheet. Initially, 1% (w/v) of NC was dispersed in ultrapure water under magnetic stirring for 30 min at room temperature. Glycerol (Sigma-Aldrich, St. Louis, MO, USA) was then incorporated as a plasticizer at 5% (w/w relative to NC dry weight) under constant agitation. Afterwards, each ZnO NPs type was added at 10% (w/w relative to NC dry weight), and homogenized for a further 30 min. Subsequently, 32 mL of each formulation was cast into 10 × 10 cm trays and dried for 48 h under controlled conditions (23 °C, 50% relative humidity). The resulting films were designed according to the incorporated nanoparticle morphology: NC/ZnO-SP, NC/ZnO-FL, and NC/ZnO-SH. Control films without nanoparticles (neat NC) were prepared under identical conditions. Films were cut into discs with a diameter of 13.5 mm for agar diffusion assay, and into 5 × 5 cm squares for antimicrobial, migration and pH assays using the model food.

All composite films were UV irradiated prior to use in antimicrobial assays to reduce surface microbial load. Films were exposed to a bank of four germicidal UV lamps (TUV G30T8, 16 W, Phillips, Amsterdam, Netherlands) with peak emission at 254 nm and an average intensity of 12.36 $Wm^{-2}$, for 10 min. To validate the efficacy of the decontamination process, UV-treated films were placed in direct contact with plate count agar (PCA) (Biokar Diagnostics, Allone, France) plates using sterile tweezers, ensuring full surface contact with the agar. The plates were incubated at 30 °C for 3 days. No microbial growth was observed during this preliminary test, confirming the effectiveness of the UV treatment in eliminating surface contamination (Fig. S2). Therefore, this decontamination step was systematically applied to all films prior to microbiological assays.

### 2.2. Characterisation of NC/ZnO NPs nanocomposite films

Valida S231C 3% and NC/ZnO composite films were characterized using a FEI QUANTA 400 FEG ESEM (FEI, Hillsboro, OR, USA)

microscope equipment, operating at an accelerating voltage of 15 kV. Prior to scanning electron microscopy (SEM) examination, the NC/ZnO films were treated with liquid nitrogen to obtain a clean cut cross-section. Additionally, films were also freeze-dried to observe the fibrillar structure and identify potential sites for ZnO NPs incorporation using a Phenom XL G2 SEM (Thermo Fisher Scientific—FEI, Eindhoven). Prior to testing, samples were frozen at −80 °C and subsequently lyophilized in a freeze dryer (LABCONCO, FreeZone, MO, USA) at −99 °C and 0.025 mbar until completely dry. The analysis was conducted at an accelerating voltage of 15 kV, and a secondary electron detector (SED) was used for micrographs capture.

The thickness of the NC/ZnO films was determined using a digital micrometer (Adamel Lhomargy, France) by randomly measuring five distinct points on each sample.

### 2.3. In vitro antimicrobial activity of NC/ZnO nanocomposite films

The antimicrobial activity of the NC/ZnO NPs films was assessed by agar diffusion assay against *Escherichia coli* ATCC 8739 *and Staphylococcus aureus* ATCC 6538P. Test bacteria were aseptically inoculated into Tryptic Soy Agar (TSA) (Biokar Diagnostics, Allone, France) plates and incubated at 37 °C for 24 h. Colonies were then harvested with a sterile loop to prepare a cell suspension in brain–heart infusion (BHI) broth (Biokar Diagnostics, Allone, France), which was incubated overnight at 37 °C to obtain a bacterial population of approximately $10^8$–$10^9$ CFU $mL^{-1}$. Subsequently, sterile swabs were immersed in each inoculum suspension and uniformly spread the suspension onto TSA plates. Film discs were then placed directly onto the inoculated plates. After incubation at 37 °C for 24 h, inhibition zones were measured and expressed in mm. The discs were then removed, and the plates were re-incubated at 37 °C, with halos monitored over a 7-day period.

### 2.4. Fresh melon sample preparation and packaging

"Pele de Sapo" melons (*Cucumis melon L.*) were purchased from a local Portuguese supermarket and selected based on ripeness, uniform peel colour, and absence of physical damage (Fig. 1a). The melons were washed with potable tap water and dried using absorbent paper. All the materials and surfaces were disinfected with ethanol, and the procedures were carried out under aseptic conditions using a Bunsen burner flame. The cleaned fruit was cut with a sterile knife into thin slices after removing the seeds and surrounding spongy tissue. Slices of approximately 10 g were prepared for microbiological analysis and approximately 2 g for migration assay. An extra set of melon slices was prepared for pH measurements. The samples were stored under refrigeration conditions (4 °C).

Previously decontaminated NC/ZnO films (5 × 5 cm) of different morphologies were used to package the melon samples, ensuring full contact between melon surface and the film at all sides of the small melon cube (Fig. 1b). The wrapped slices were then placed inside sterile bags and stored under refrigeration conditions (Fig. 1c). Microbial, migration, and pH analyses were conducted at five different time points over the course of one week. Triplicate analyses were performed for each nanocomposite type: NC/ZnO-SP, NC/ZnO-FL, NC/ZnO-SH and NC control.

#### 2.4.1. Microbiological analyses

Total mesophilic aerobic counts at 30 °C and psychrotrophic counts at 7 °C, *Enterobacteriaceae*, and yeast and mould populations were evaluated at days 0, 3, 5, 6, and 7 of the storage period. Under sterile conditions, the NC film was removed from the melon, and a 10 g portion of the slice was homogenized for 30 s with 90 mL of Ringer's solution (Biokar Diagnostics, Allone, France) using a Stomacher SMASHER® Sample Blender (bioMérieux, Marcy-l'Étoile, France). Serial dilutions were prepared in Ringer's solution as required for microbial enumeration. PCA was used for total mesophilic aerobic counts (incubated at 30 °C for 3 days), and for psychrotrophic counts (incubated at 7 °C for 10 days). *Enterobacteriaceae* were quantified using RAPID' *Enterobacteriaceae* Agar (Bio-Rad Laboratories, Marnes-la-Coquette, France) after incubation at 37 °C for 24 h. Yeasts and moulds were enumerated on Dichloran Rose Bengal Chloramphenicol (DRBC) agar (Biokar Diagnostics, Allone, France) following incubation at 25 °C for 5 days. A melon sample without film was used as a control. All microbial counts were expressed as log colony-forming units per gram of sample (log CFU $g^{-1}$).

#### 2.4.2. Zinc migration analyses

The migration of Zn from NC/ZnO nanocomposite films into melon was assessed over a storage period of 8 days. Fresh-cut melon samples were collected after 0, 1, 3, 5, and 8 days for the Zn determination. The Zn concentration was quantified by flame AAS according to standard EN 14084, following microwave digestion of the whole melon cube. A realistic scenario was considered, based on the actual surface area-to-mass ratio (A/M) for half a melon (Fig. S3).

Microwave digestion of 2 g of melon was performed in digestion vessel with the addition of 5 mL of suprapur nitric acid 65% (Panreac, Barcelona, Spain). The samples were then processed using a microwave digestion system (Speedwave MWS-3+, Berghof, Germany), according to the program detailed in Table 1. Upon completion of the microwave treatment, the digested samples were diluted with ultrapure water to a

**Table 1**
Microwave digestion program.

| Stage | 1 | 2 | 3 | 4 | 5 |
|---|---|---|---|---|---|
| **T (°C)** | 130 | 170 | 200 | 100 | 100 |
| **Pressure (bar)** | 20 | 20 | 20 | 20 | 20 |
| **Time (min)** | 5 | 10 | 15 | 2 | 2 |
| **Ramp (min)** | 5 | 5 | 1 | 5 | 1 |
| **Power (watt)** | 30 | 40 | 50 | 30 | 20 |


**Fig. 1.** – Experimental procedure with melon samples: a) whole melon fruits purchased from a local Portuguese supermarket; b) melon slice (~3 × 3 cm) wrapped with the NC/ZnO film (5 × 5 cm); c) wrapped samples corresponding to one of the five experimental time points, stored in sterile bags for subsequent analysis.

final volume of 50 mL and subsequently analysed by AAS.

Zinc quantification was performed using a flame AAS (PerkinElmer Aanalyst 400, Waltham, MA, USA), equipped with a zinc hollow cathode lamp at a wavelength of 213.9 nm. Measurements were carried out using an air–acetylene flame under standard operating conditions recommended by the manufacturer. Zinc working standard solutions with 1 % (v/v) $HNO_3$, ranging from 0 to 0.50 mg $L^{-1}$, were prepared from a 1000 mg $L^{-1}$ standard stock solution to obtain a calibration curve. Five replicate measurements were performed for each sample and working solution. System performance was assessed by determining the limit of detection (LOD: 0.008 mg $L^{-1}$), the limit of quantification (LOQ: 0.025 mg $L^{-1}$), and recovery (90 - 110%). When necessary, samples were further diluted with ultrapure water to ensure that the absorbance signal was within the specified Zn concentration range.

#### 2.4.3. pH determination

Melon samples were collected on days 0, 1, 3, 5, and 7 for pH determination. The samples were removed from the cold storage, the NC films carefully removed from the slices and the measurements were taken after 3 min at room temperature. The pH of the melon slices was measured using a solid-state pH meter (Mettler Toledo, SevenDirect SD50, Greifensee, Switzerland).

### 2.5. Data handling and statistical analysis

Statistical analysis was performed using IBM SPSS Statistics (version 28), GraphPad Prism (version 10.6.1), and Microsoft Excel. Results were presented as mean ± standard deviations using tables and graphic representations.

One-way analysis of variance (ANOVA) followed by Fisher's least significant difference (LSD) post hoc tests was used to compare inhibition zone diameters among film groups for each microorganism. For the one week experiments (microbiological analysis, Zn migration and pH evaluation), two-factor ANOVA was applied, with storage time (days) and packaging condition (melon control, NC control, NC/ZnO-SP, NC/ZnO-SH, NC/ZnO-FL) as factors. Tuckey's and LSD post hoc tests were used to identify statistically significant differences between each factor. A two-sided $p < 0.05$ was considered statistically significant.

## 3. Results and discussion

### 3.1. Characterisation of NC/ZnO films

SEM micrographs of the Valida S231C 3% cellulose are represented in Fig. 2. Fig. 2a and b reveal a relatively homogeneous structure, with fine and long interconnected fibres forming a dense, entangled network. SEM micrographs of the freeze-dried NC matrix show an open, highly porous network composed of interconnected cellulose fibres (Fig. 2c and d). The voids and fibre intersections serve as potential sites for ZnO NPs incorporation, enabling their dispersion within the matrix.

After incorporating ZnO NPs into the NC matrix, cross-section SEM micrographs of the NC-based films were obtained to evaluate the distribution of ZnO NPs and their impact on the overall film structure (Fig. 3). The neat NC film exhibits a compact and homogeneous structure, with no visible particles (Fig. 3a and b). This control serves as a reference to assess the structural modifications induced by ZnO NPs incorporation. Regarding the NC/ZnO-SP composite film (Fig. 3c and d), the presence of ZnO NPs is evident, but their distribution appears somewhat uneven, with regions showing higher particle concentration. This may indicate partial aggregation of the ZnO NPs within the cellulose matrix. In contrast, the NC/ZnO-FL film (Fig. 3e and f) exhibits a more homogeneous dispersion of ZnO NPs, with the particles appearing to be better distributed throughout the matrix. The micrographs suggest that ZnO NPs are not only embedded within the NC fibres but also deposited on the surface. Regarding NC/ZnO-SH (Fig. 3g and h), NPs appear to be well distributed across both the surface and internal regions of the film, with some small particle clusters observed within the layered NC structure. All the films present a torn, layered appearance as they were not rigid enough to fracture cleanly. Nevertheless, this did not hinder the observation of the internal structure and particle distribution.

ZnO NPs embedded in the matrix might be bound to the hydroxyl groups of cellulose fibres through hydrogen bonding (Ghule et al., 2006). Comparing the ZnO-loaded films with the neat NC film, it is evident that ZnO NPs incorporation influences the cellulose matrix: an increase in porosity can be observed within the NC network, potentially leading to greater inter-fibre spacing. Additionally, the formation of ZnO NPs clusters in certain regions may introduce structural irregularities

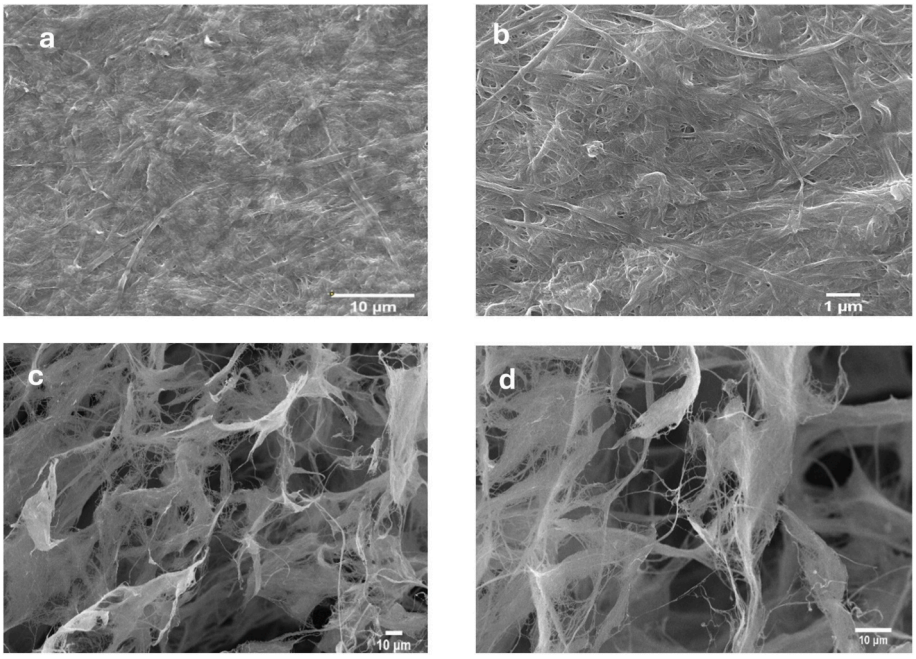


**Fig. 2.** SEM micrographs of the NC matrix surface at magnifications of (a) 5 000x and (b) 20 000x; and after freeze-drying process at magnifications of (c) 2 050x and (d) 4 300x.

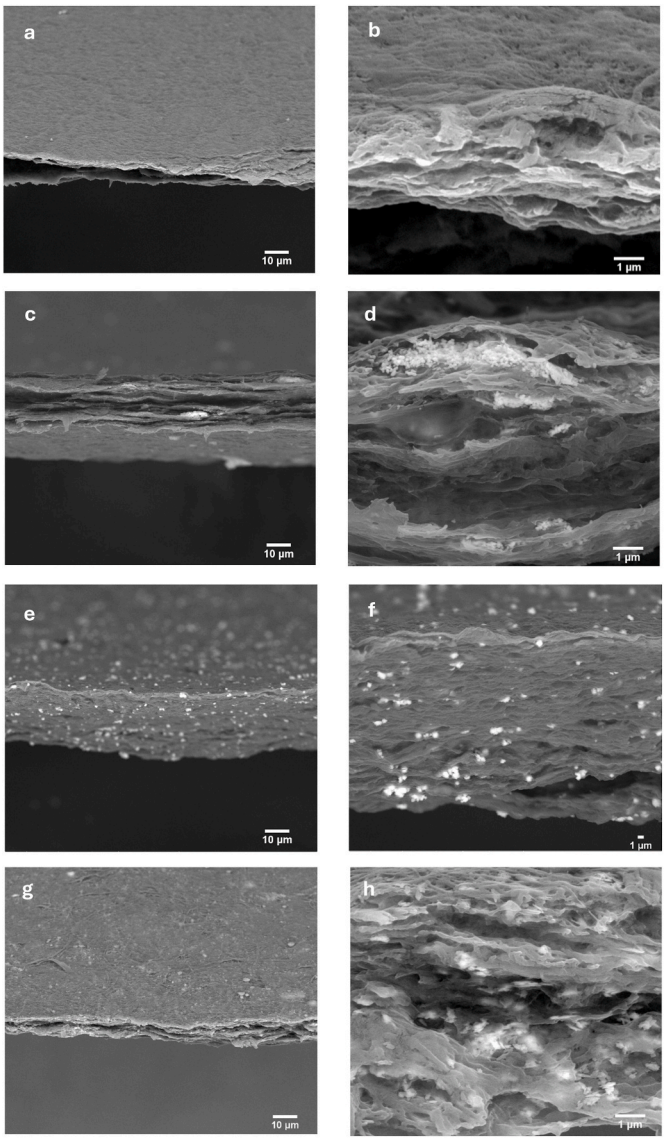


**Fig. 3.** Cross-section SEM micrographs of the films: NC (a, b), NC/ZnO-SP (c, d), NC/ZnO-FL (e, f), and NC/ZnO-SH (g, h). Magnifications: 2 000x (a, c, e, g); 5 000x (f); 25 000x (b, d, h).

that could influence the mechanical integrity of the films. Abbas et al., 2019 reported that a uniform distribution of nanoparticles is crucial for enhancing mechanical properties, whereas aggregation can lead to decreased flexibility and potential defects in the composite structure.

The interaction between ZnO NPs and the cellulose matrix is also crucial for evaluating Zn migration. Uniform dispersion of ZnO NPs with strong bonding to the matrix can lead to lower migration rates. In contrast, higher aggregation can alter the structural integrity of the composite, potentially enabling nanoparticle migration (Babakhani, 2019). Furthermore, in areas where ZnO NPs are more exposed to the film surface, a higher release of ZnO over time may be expected. Studies have reported that the extent of NPs exposure on the film's surface plays a significant role in Zn migration behaviour (Bumbudsanpharoke et al., 2019). Excellent compatibility and miscibility between the NC matrix and the filler materials were also observed in cellulose nanofiber-based composite films reinforced with zinc oxide nanorods and grapefruit seed extract (Roy et al., 2021).

The thickness of neat NC was 29.6 ± 1.1 μm, which slightly increased upon the incorporation of ZnO NPs. Among the samples, NC/ZnO-SH exhibited the highest thickness value (42.0 ± 4.0 μm), compared to the films with spherical (33.4 ± 4.2 μm) and flower-shaped (32.4 ± 2.5 μm) ZnO NPs incorporation. This increase confirms that the incorporation of fillers into the film matrix influences its thickness, as previously reported (Ahmadi et al., 2021). This trend aligns with prior findings, in which the incorporation of ZnO NPs into chitosan-based films resulted in a gradual increase in thickness from 42.0 μm to 59.3 μm, depending on the ZnO NPs concentration (Souza et al., 2021). Another study reported that incorporating $Fe_3O_4$ NPs into the cellulosic matrix increased the distance between cellulose fibres in the cross-section of the films, thereby increasing film thickness (Furlan et al., 2019).

### 3.2. Antimicrobial activity of NC/ZnO nanocomposite films

The antimicrobial activity of the different NC/ZnO films was evaluated against gram-negative *E. coli* and gram-positive *S. aureus* using an agar diffusion assay. The results are presented in Table 2 and Fig. 4. Incorporation of ZnO NPs into NC films enhanced antimicrobial efficacy compared to neat NC, particularly against *S. aureus*, although the magnitude of the effect depended on nanoparticle shape.

Among the tested morphologies, sheet-shaped ZnO NPs produced the strongest inhibitory effect against both bacteria, followed by spherical shape; flower-like particles showed only limited or negligible effect. For *S. aureus*, the NC/ZnO-SP and NC/ZnO-SH films produced inhibition zones of 20.5 ± 1.0 and 21.8 ± 1.2 mm, respectively, compared with 17.1 ± 4.2 mm for the NC control. In contrast, the NC/ZnO-FL film produced a smaller inhibition zone (16.1 ± 1.0 mm) than the control. Statistical analysis revealed overall differences among films (one-way ANOVA, $p < 0.05$). NC/ZnO–SH films showed significantly larger inhibition zones than neat NC (Fisher's LSD test, $p < 0.05$). Conversely, NC/ZnO–FL films produced significantly smaller zones than both NC/ZnO–SP and NC/ZnO–SH (Fisher's LSD test, $p < 0.05$), indicating lower antibacterial efficacy against *S. aureus*. Although neat NC films exhibited initial antimicrobial activity, bacterial regrowth was observed within the inhibition zone upon disc removal after 48 h, indicating that the effect was not maintained. In contrast, inhibition zone corresponding to the films containing ZnO NPs maintained clear and stable aspect for at least 7 days, confirming their long-term antimicrobial performance.

For *E. coli*, NC/ZnO-SH and NC/ZnO-SP films produced the largest inhibition zones (17.5 ± 0.3 and 16.9 ± 1.1 mm, respectively), while NC/ZnO-FL and neat NC film produced smaller zones (11.4 ± 5.6 and 10.5 ± 5.4 mm, respectively). However, differences among films were not statistically significant (one-way ANOVA, $p = 0.126$). After disc removal, no bacterial regrowth was observed in any inhibition zone, including those produced by the NC control, for at least 7 days. This apparent absence may be partially influenced by the hygroscopic and adhesive nature of NC, which can retain moisture and physically entrap bacterial cells, thereby potentially preventing the visualization of colonies (Solhi et al., 2023). Another possible explanation is a baseline antimicrobial activity of the neat NC film, attributed to the presence of the 1,2-Benzisothiazolin-3-one, a cellulose dispersion additive with well-documented antimicrobial properties against bacteria, fungi, and yeast (Liu et al., 2025; Viani et al., 2017). Incorporating ZnO NPs, especially those in the SH and SP morphologies, further enhanced the effect, resulting in larger and more uniform inhibition zones.

**Table 2**
Antimicrobial activity of NC/ZnO films determined by agar diffusion assay. Results are expressed as inhibitory halos (mm).

| Microorganism | Neat NC | NC/ZnO-SP | NC/ZnO-SH | NC/ZnO-FL |
|---|---|---|---|---|
| *S. aureus ATCC 6538P* | 17.1 ± 4.2 | 20.5 ± 1.0 | 21.8 ± 1.2 | 16.0 ± 1.0 |
| *E. coli ATCC 8739* | 10.5 ± 5.4 | 16.9 ± 1.1 | 17.5 ± 0.3 | 11.4 ± 5.6 |

Values represent the mean ± SD of three independent experiments, each performed in technical triplicate (three discs per plate; two diameter readings per disc).

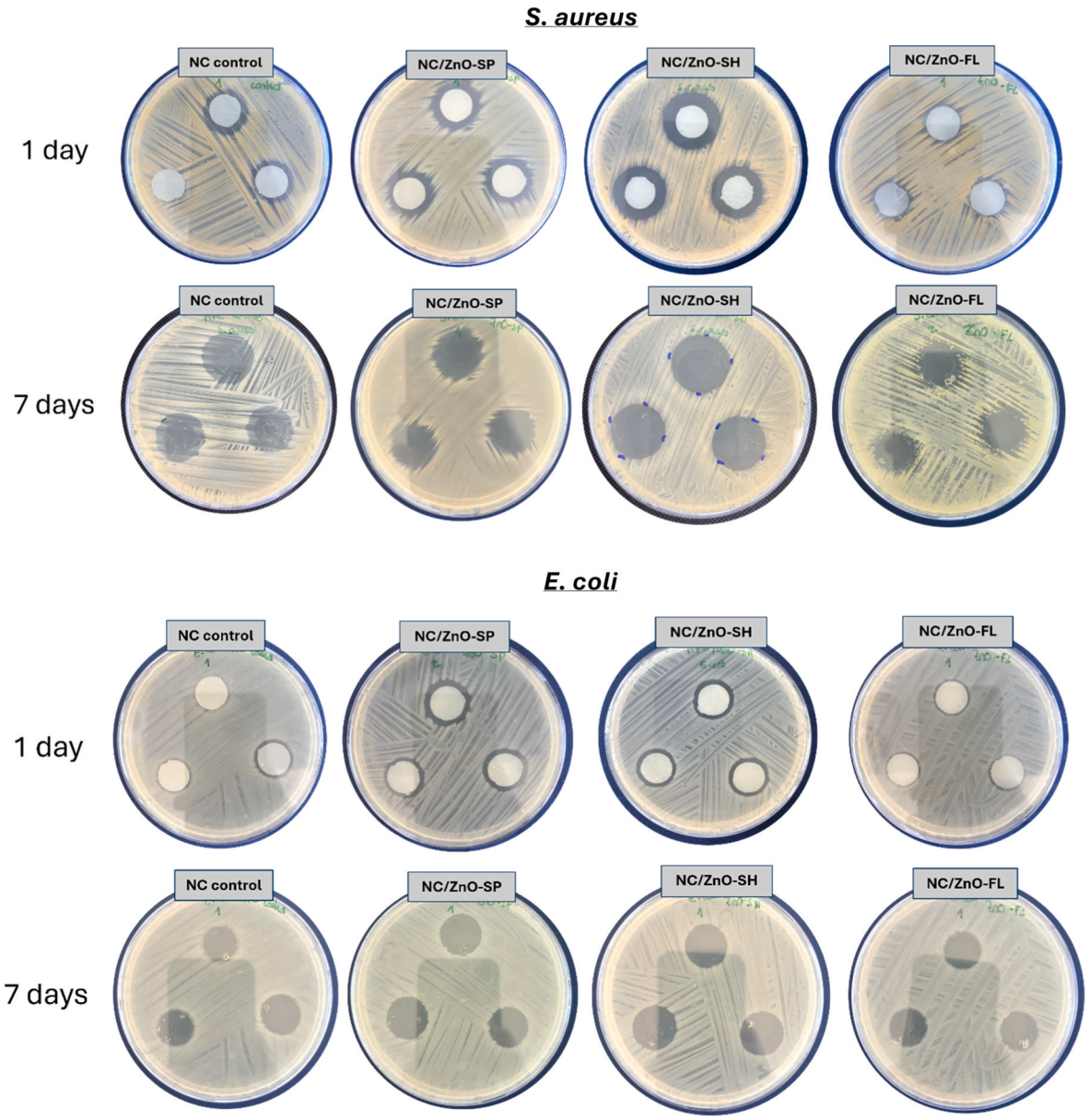


**Fig. 4.** – Agar diffusion assay of NC/ZnO films against *S. aureus* and *E. coli* after 24 h of incubation and 7 days after disc removal.

These findings are consistent with previous reports on ZnO NPs tested in suspension (Mendes et al., 2024, 2025), in which SP and SH morphologies demonstrated superior antimicrobial activity compared with FL. When incorporated into NC films, however, the ZnO-FL antibacterial effect was almost completely suppressed, suggesting that the NC matrix plays a critical role in modulating ZnO antimicrobial activity. Notably, in some cases NC/ZnO-FL films even displayed smaller inhibition zones than neat NC, indicating that the presence of FL particles may also attenuate the intrinsic antimicrobial activity of the NC matrix. This effect could arise from the three-dimensional geometry of FL particles, which may become entrapped within the fibrillar cellulose network, thereby hindering the diffusion of antimicrobial agents. Such interference may affect not only the release of $Zn^{2+}$ ions and ROS from the FL particles, but also the diffusion of compounds inherently present in neat NC (benzisothiazolinone). Indeed, our previous work demonstrated that ZnO-FL possesses a significantly lower specific surface area compared with ZnO-SP and ZnO-SH particles (Mendes et al., 2024), further supporting their reduced antimicrobial performance. In contrast, SP and SH nanoparticles offer great surface area and more efficient $Zn^{2+}$/ROS release, which explains the larger inhibition zones observed.

In this study, *S. aureus* (gram-positive) was more susceptible to ZnO NPs than *E. coli* (gram-negative). This difference is likely due to the structural differences in their cell walls, as the outer lipopolysaccharide membrane of gram-negative bacteria acts as an additional barrier that limits the penetration of antimicrobial agents, such as $Zn^{2+}$ ions and ROS (Babayevska et al., 2022). This trend contrasts with our previous findings in suspension (Mendes et al., 2025), where freely dispersed ZnO NPs produced greater activity against *E. coli* than against *S. aureus*. In suspension, rapid $Zn^{2+}$ release, enhanced particle–cell interactions, and ROS generation likely account for the stronger effect on *E. coli*, which is often more vulnerable to oxidative stress (Behera et al., 2024). However, when ZnO NPs are embedded in NC films, nanoparticle mobility and ion release are restricted, and the diffusion-based nature of the agar assay further limits the availability of antimicrobial agents. Under these conditions, the outer membrane of *E. coli* may provide additional protection, while *S. aureus*, lacking this outer layer, is comparatively more affected. Similar findings have been reported for bacterial cellulose films incorporated with ZnO NPs (Shahmohammadi Jebel & Almasi, 2016),

although that study used commercial particles and did not examine NPs morphology. In contrast, in the present study the NC control exhibited some baseline antimicrobial activity, which may have influenced the comparative outcomes.

### 3.3. Shelf life evaluation of fresh melon packaged with NC/ZnO films

#### 3.3.1. Microbial growth monitoring

To evaluate the applicability of NC/ZnO films as a packaging material for extending food shelf life, microbiological analyses were performed on fresh-cut melon samples stored at 4 °C for 7 days. As expected, both the melon control and the neat NC control showed increasing microbial counts during storage, with counts consistently higher than those observed for melons packaged with NC/ZnO films across all microbial groups (Fig. 5). Notably, the melon with NC control exhibited approximately 1 log CFU $g^{-1}$ higher microbial counts than the melon control alone. Although neat NC films displayed antimicrobial activity in the agar diffusion assay, likely due to the presence of 1,2-Benzisothiazolin-3-one, this effect was not evident in the melon storage tests, where microbial growth was even more pronounced. This apparent divergence can be attributed to differences between the two experimental systems. In the agar diffusion assay, antimicrobial compounds can easily diffuse through the agar medium because of its simple matrix nature, facilitating the formation of inhibition zones. In contrast, in real food systems such as fresh-cut melon, the diffusion of such compounds from the film to food surface may be limited. In fact, the composition of the melon is a complex interaction of carbohydrates, fibers, minerals, etc. Additionally, the NC film may reduce surface water loss and maintain a more humid environment around the melon surface, which can favour microbial proliferation (Ahmad & Siddiqui, 2015). Furthermore, interactions with the natural microbiota of melon may reduce the effectiveness of weak antimicrobial compounds. Together, these factors may mask the intrinsic antimicrobial effect observed for neat NC.

Melon samples packaged with NC/ZnO films exhibited a clear reduction in microbial growth throughout storage, confirming the antimicrobial efficacy of the ZnO-containing films. However, the magnitude of this effect strongly depended on nanoparticle morphology. NC/ZnO-SH films were the most effective, maintaining the lowest microbial counts, followed by spherical particles, while flower-shaped particles exhibited only limited activity. These results are consistent with the agar diffusion assay and with previous reports on ZnO NPs tested in suspension (Mendes et al., 2024, 2025), in which SP and SH morphologies demonstrated superior antimicrobial activity, whereas FL displayed poor antimicrobial performance.

Initial populations of total mesophilic aerobic bacteria at 30 °C and 7 °C were approximately 2 and 1 log CFU $g^{-1}$, respectively, while *Enterobacteriaceae* as well as yeasts and moulds were below the detection limit, indicating the good initial microbiological quality of the fresh-cut melon. For total aerobic counts at 30 °C and 7 °C (Fig. 5a and b), both storage time and packaging condition had a statistically significant effect on microbial counts ($p < 0.05$). However, the interaction between the two factors was only significant at 30 °C. Counts steadily increase in the control samples, reaching values close to or above $10^5$ CFU $g^{-1}$ by day 7, which corresponds to the upper acceptability limit for fresh-cut fruits (INSA, 2019; Oms-Oliu et al., 2010). In contrast, melon samples packaged with NC/ZnO films exhibited lower counts throughout storage. At 30 °C, all ZnO films resulted in statistically significant reductions in counts on day 7 compared with the cellulose control ($p < 0.05$). In particular, NC/ZnO-SH films were the most effective, with final counts of approximately $10^2$ CFU $g^{-1}$, which were significantly lower than those of all other study groups (controls and the other ZnO films, $p < 0.05$). On the other hand, NC/ZnO-FL initially delayed microbial proliferation (at day 3, compared with NC control, $p < 0.05$), but this effect was not sustained, and by day 7, they displayed the highest microbial loads among the three morphologies, confirming their poor antimicrobial performance. At 7 °C (Fig. 5b), the control groups (melon and NC film) were significantly higher than the ZnO-containing film groups ($p < 0.05$).

*Enterobacteriaceae* became detectable in the control samples after day

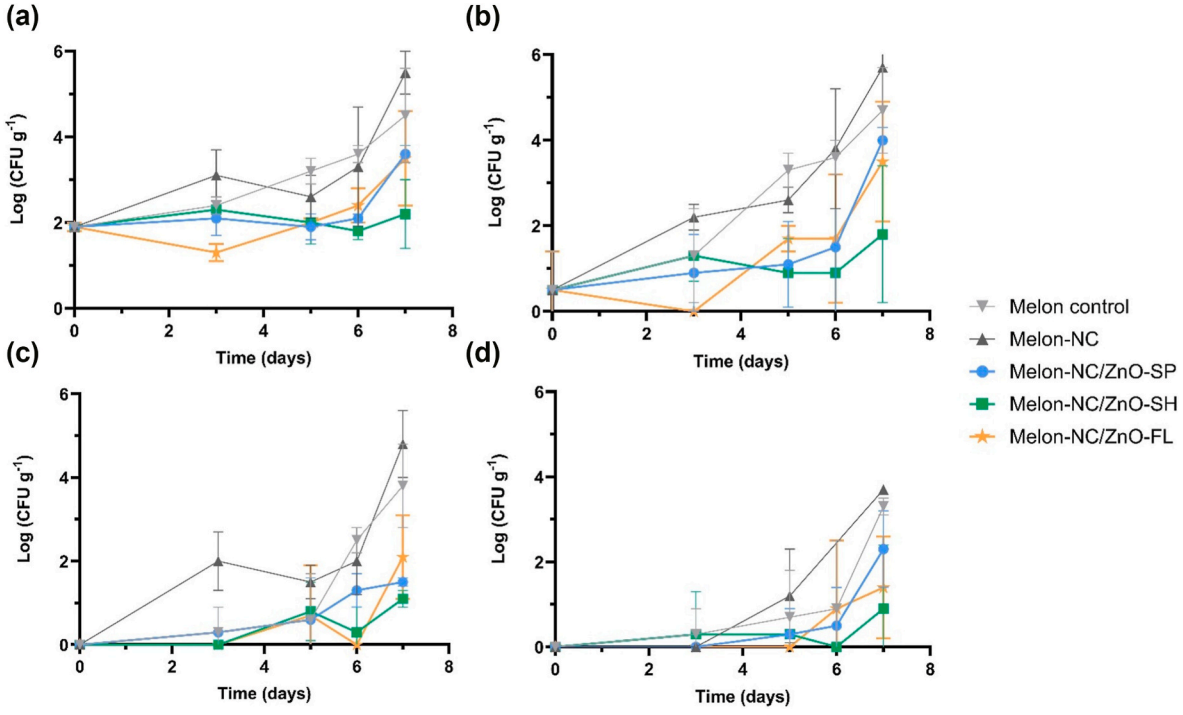


**Fig. 5.** Microbial counts of fresh-cut melon samples stored at 4 °C for 7 days: a) total aerobic counts at 30 °C, b) total aerobic counts at 7 °C, c) *Enterobacteriaceae*, and d) yeasts and moulds. Samples include melon control, NC film control, and NC films containing ZnO NPs (SP, SH, FL). Results are expressed as mean ± standard deviation (n = 3) and reported as log CFU $g^{-1}$.

3 and increased sharply until the end of storage (Fig. 5c). In the NC/ZnO films, detectable viable microorganisms appeared later during storage, and the microbial growth increased more slowly, remaining lower than in the controls. The interaction between packaging condition and storage time for *Enterobacteriaceae* counts was significant ($p < 0.05$). Higher counts were observed in melon packaged with NC films, reaching values of $10^5$ CFU $g^{-1}$ by day 7, which corresponds to the upper acceptability limit for fresh-cut fruits. According to microbiological guidelines, satisfactory levels of *Enterobacteriaceae* should remain below $10^4$ CFU $g^{-1}$ (INSA, 2019; Oms-Oliu et al., 2010). In contrast, populations remained very low or undetectable in melons packaged with NC/ZnO films, particularly with the SH morphology. On day 7, differences were observed for all three ZnO morphologies compared with both melon and NC controls ($p < 0.05$). Although *Enterobacteriaceae* are primarily used as hygiene indicators (relevant to initial contamination and processing), their marked inhibition during storage is also important because members of this group include potential foodborne pathogens (Schwan et al., 2022).

Yeasts and moulds also showed progressive growth in the control samples, reaching approximately 4 log CFU $g^{-1}$ after 7 days, whereas their proliferation was significantly reduced in the presence of ZnO-containing films (Fig. 5d). There were no statistically significant differences in counts across packaging groups, nor any interaction between time and packaging groups. However, the effect of time showed that after one week, yeast and mould counts were significantly higher than at earlier time points ($p < 0.05$). According to microbiological guidelines, counts below $10^4$ CFU $g^{-1}$ are considered satisfactory, and all samples complied with this limit throughout the 7-day storage period (INSA, 2019; Oms-Oliu et al., 2010). Yeasts and moulds are generally present at lower levels than total mesophilic aerobic bacteria in fresh-cut melon, as previously reported by Ukuku et al., 2018, which is consistent with the trends observed in the present study.

In a previous study, cellulose-based absorbent pads containing silver nanoparticles, instead of ZnO-NPs, were applied to fresh-cut melon (Fernández et al., 2010). In that work, microbial growth in melon pieces was only moderately reduced: approximately 0.8 log CFU $g^{-1}$ for total aerobic counts at 30 and 7 °C. This can be explained by the indirect contact of the silver-loaded pads with the fruit, as they became active mainly after being impregnated with melon exudates, thereby limiting their direct antimicrobial effect on the fruit surface. In contrast, the NC/ZnO films in the present study remained in continuous contact with the melon, leading to greater reductions in microbial counts. Similar antimicrobial trends in fresh-cut melon have been reported when incorporating silver NPs into other biopolymeric matrices, such as chitosan (Ortiz-Duarte et al., 2019) and alginate (Danza et al., 2015). However, the magnitude of microbial inhibition varied depending on the polymer and nanoparticle type.

The stronger antimicrobial effect observed in this study, particularly for the ZnO-SH films, can be explained by the multiple antimicrobial mechanisms of ZnO NPs. These include the release of $Zn^{2+}$ ions, the generation of ROS, which induce oxidative damage to cellular components, and the direct contact of nanoparticles with microbial membranes, leading to structural disruption. The superior performance of the SH morphology can be attributed to its higher specific surface area, and the continuous contact of the films with the melon surface likely promoted enhanced $Zn^{2+}$ release and ROS generation, thereby reinforcing their antimicrobial activity (Mendes et al., 2024). In contrast, FL showed lower surface area and poorer complex interactions with the matrix, reducing ion/ROS flux and direct cell contact.

In summary, these results clearly demonstrate that the incorporation of ZnO NPs delays microbial proliferation in fresh-cut melon, thereby extending its microbiological shelf life. NC/ZnO-SH films effectively maintained safe microbial levels for at least 7 days under refrigerated storage, whereas control samples reached the upper acceptability limit within 3–4 days. These findings highlight the potential of ZnO-containing cellulose films as active packaging materials to improve food safety, prolong shelf life, and reduce food waste in minimally processed fruits.

### 3.3.2. *Evaluation of zinc migration in packaged melon*

Zinc migration from NC/ZnO nanocomposite films into melon was assessed under realistic conditions. The results showed that melons in contact with all NC/ZnO films exhibited a similar migration profile, characterized by a rapid increase during the initial days of storage, followed by a stabilization after day 4 (Fig. 6). This trend suggests an initial fast diffusion of loosely bound or surface-available Zn species, followed by the establishment of equilibrium between the film and food matrix. Although the three morphologies exhibited distinct particle sizes and specific surface areas, as represented in Fig. S1, these differences did not influence Zn migration in the melon matrix. In fact, ZnO NPs morphology can influence dissolution behaviour, as smaller particles with higher surface areas tend to release more $Zn^{2+}$ ions. However, under the present conditions, the migration process appears to be governed primarily by the properties of the food matrix rather than by NPs morphology. The high water content of melon may promote ZnO dissolution and $Zn^{2+}$ release in a similar pattern for all the samples, regardless of NPs and morphology.

The SML for Zn (5 mg $kg^{-1}$ of food) was reached after approximately 2 days, with concentrations further increasing to 7 - 8 mg $kg^{-1}$ melon. These levels exceeded the migration limit, underscoring the importance of carefully controlling the interaction between ZnO NPs and the food matrix, as balancing antimicrobial efficacy with regulatory compliance is essential for the safe application of such materials in food packaging. It is important to note that the experimental setup represents a high contact surface area scenario, involving direct exposure of a small melon portion to a relatively large film area, which increases migration compared to typical packaging conditions. Therefore, these results should not be interpreted as an automatic disqualification of ZnO nanocomposites for food packaging applications. These findings represent a worst-case scenario and underscore the need for further optimization of overall packaging, considering that Zn migration behaviour strongly depends on several factors, including NPs loading, NPs/matrix interaction, food composition, storage time, temperature, and the surface area-to-mass ratio between packaging and food.

The control melon samples exhibited negligible Zn levels throughout the storage period, confirming that the detected Zn was originated from nanocomposite films. Two-way ANOVA revealed statistically significant interaction between storage time and packaging condition groups ($p < 0.05$) on Zn migration. Interaction post-hoc Tukey's test showed that, from day 1 onwards, all melons containing NC/ZnO NPs films exhibited significantly higher Zn levels compared to the control ($p < 0.05$), and no significant differences were observed among the different ZnO film morphologies at any time point.

The experimental Zn concentration data (Table S2) were converted

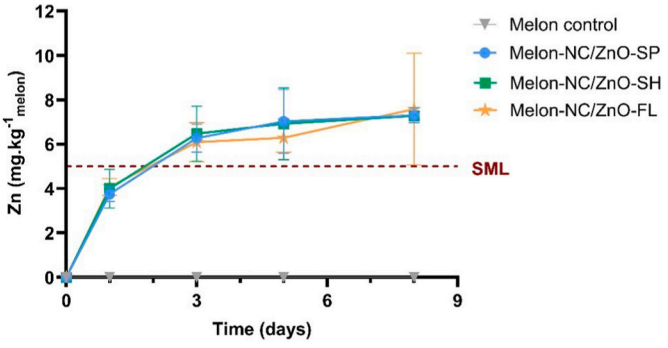


**Fig. 6.** – Zn migration from NC/ZnO nanocomposite films into fresh-cut melon during storage at 4 °C for 8 days, under a realistic scenario (A/M = 1 $dm^2$ $kg^{-1}$ food). Results are expressed as mean ± standard deviation (n = 3) and reported as mg $kg^{-1}$ melon. The SML (5 mg $kg^{-1}$) food is indicated for reference.

to realistic packaging conditions based on the actual surface area-to-mass ratio of a half melon. Average melon dimensions of 25 × 15 cm and a total weight of 4 kg per fruit (2 kg per half fruit) were considered. The edible portion was assumed to extend 4 cm from the surface. After subtracting the seed cavity, the effective contact area was estimated as 2 $dm^2$. Normalized to the mass of 2 kg, this corresponded to an A/M ratio of 1 $dm^2\ kg^{-1}$ (Fig. S3). The detailed calculation is provided in supplementary material. No previous studies on packaged melon have assessed the migration of compounds directly to the fruit itself. One study developing cellulose pad with silver NPs demonstrated silver migration into an external medium (Mueller-Hinton Broth) using graphite-furnace atomic absorption spectrometry, rather than directly into the melon matrix (Fernández et al., 2010).

The Zn migration profiles observed in melon differed from those previously reported for the same films tested with food simulants (water and 10% ethanol) (Mendes et al., 2026). Higher Zn migration rates were observed in the real food matrix than in food simulants. In water food simulant, the SML was reached only after 29 days, and Zn levels approached 8 mg $kg^{-1}$ after 35 days. In contrast, melon samples reached similar Zn concentrations after only 8 days of storage. Moreover, when using food simulants, a clear difference in Zn migration was observed among the three ZnO morphologies, whereas in melon, all samples exhibited similar migration behaviour. In fact, melon has a complex composition, including organic acids, sugars, high water content, and enzymatic activity, that may facilitate ZnO dissolution and $Zn^{2+}$ release (Youn & Choi, 2022). Studies with ZnO NPs incorporated in bacterial nanocellulose have also demonstrated that Zn migration was much higher in chicken food than in ethanolic food simulants (Soares Silva et al., 2023). This discrepancy highlights the limitations of simulant-based testing as models of real food interactions, although such approaches remain important for regulatory compliance when overestimation is assured (Lerch et al., 2023). It is important to note that migration levels in real foods are expected to vary depending on food type, storage conditions, packaging characteristics, and intrinsic food properties, such as composition, water content, and pH. Under realistic exposure conditions, Zn migration from NC/ZnO films can approach or surpass regulatory migration limits, especially in high-moisture and acidic food matrices. Future studies should therefore extend to different food matrices and packaging systems to better understand the NPs migration variation under real case scenarios. Considering the relatively high Zn concentrations observed in melon, future strategies could also include the application of surface coatings or barrier layers designed to delay Zn migration.

Another aspect to consider is that the present study addressed only total Zn migration, without differentiating between ionic $Zn^{2+}$ and nanoparticulate forms. Based on previous results, also for NC films, obtained with food simulants, ca 18% of the total migrated Zn corresponded to ZnO NPs (Mendes et al., 2026). As a rough estimation, a similar ratio can be considered for melon samples. Considering the total Zn migration values of approximately 8 mg $kg^{-1}$ melon, this corresponds to an estimated 1.3 – 1.5 mg $kg^{-1}$ potentially attributed to ZnO NPs, while the remaining proportion would represent the ionic $Zn^{2+}$. However, this estimation should be interpreted with caution, as the complex composition of melon (organic acids, sugars, enzymes) may influence ZnO dissolution and migration dynamics, leading to a different ionic/nanoparticle ratio compared with that of food simulants. Differentiating between these two migrating forms is essential for accurate assessment of potential exposure and toxicity, since physicochemical properties, mechanisms and bioavailability of $Zn^{2+}$ ions differ from those of ZnO NPs (EFSA, 2021; Wu et al., 2019). This distinction remains one of the major analytical challenges in the field, as well as regulation gap regarding nanoparticle migration (Ansari et al., 2026). Understanding the type of migration and the release mechanisms is indeed crucial for future toxicological evaluations of these materials.

### 3.3.3. Monitoring of pH in packaged melon

One crucial parameter related with microbiological and Zn migration results was the pH evolution of fresh-cut melon in contact with NC/ZnO films, stored at 4 °C for 7 days. Results for melon control and melon with nanocomposite films are shown in Fig. 7. The initial pH of 6.5 exhibited a sharp decrease on the first day, followed by stabilization until day 7 for all the samples. This initial pH drop may be associated with physiological responses triggered by tissue disruption during cutting, which can induce stress and accelerate metabolic processes in fresh-cut fruits, thereby masking the immediate effect of the packaging (Guo et al., 2023). The subsequent observed fluctuations may be attributed to intrinsic variability of the melon metabolic activity, as well as the experimental measurements. Both melon control and the melon-NC control demonstrated a stronger decrease (to approximately 5.8), whereas melons packaged with NC/ZnO films maintained slightly higher pH values after 7 days. Two-way ANOVA showed that storage time and packaging condition significantly affected melon pH values ($p < 0.05$), while their interaction was not significant. Post-hoc Tukey's test revealed that melon packaged with NC control film exhibited significantly lower pH compared to melons packaged with NC/ZnO films ($p < 0.05$). The more acidic pH observed in the control samples can be explained by the higher microbial activity (Fig. 5), since proliferation of microorganisms producing organic acids and other metabolites contribute to pH reduction and accelerate fruit spoilage. In contrast, melons packaged with ZnO films maintained slightly higher pH values, likely due to microbial growth inhibition. Furthermore, pH is also a key factor influencing ZnO solubilization, as lower pH may promote dissolution and the subsequent release of $Zn^{2+}$ ions (Hakeem et al., 2020). The gradual pH decrease observed over one week may therefore contribute for the increased Zn migration in melons packaged with NC/ZnO films (Fig. 6).

A similar behaviour of an initial pH decline has been reported for fresh-cut melon fruit packaged with chitosan/graphene oxide films (Paiva et al., 2020). However, that study extended storage to 21 days, revealing a subsequent pH increase after the initial decline, which was not seen in the current work. This implies that multiphase dynamics may influence pH change based on storage duration and microbial activity. In food science, pH is a crucial quality parameter as it influences various aspects such texture, flavour, and microbial stability, while also serving as an indicator of food safety (Venkatesan & Muniyan, 2024). Nevertheless, the intrinsic characteristics of the food matrix, such as water activity and sugar content, can strongly influence the pH evolution. Additionally, extrinsic factors such as initial microbial load and storage conditions can also significantly affect these dynamics. As a result, the present outcomes cannot be directly generalized to other food matrices and should instead be evaluated on a case-by-case basis, considering their specific physicochemical and microbiological properties.

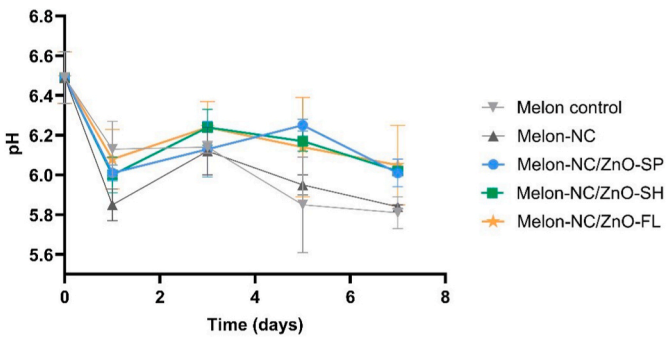


**Fig. 7.** – Evolution of pH in fresh-cut melon samples stored at 4 °C for 7 days. Samples include melon control, NC film control, and NC films containing ZnO NPs (SP, SH, FL). Results are expressed as mean ± standard deviation (n = 3).

## 4. Conclusion

This work allowed for the development and evaluation of NC films containing three different ZnO NPs morphologies, assessing their capacity to extend melon shelf life, by reducing microbial proliferation, in parallel with zinc migration assessment.

SEM micrographs confirmed the nanofibrillar and porous NC network of the films, suggesting an appropriate structure for ZnO NPs linking, and cross-sectional SEM showed the distribution of the ZnO NPs within the matrix. *In vitro* antimicrobial activity of NC/ZnO films was assessed against *S. aureus* and *E. coli,* where results revealed a clear morphology effect: NC/ZnO–SH produced higher inhibitory halos, followed by NC/ZnO-SP, whereas FL films showed lower inhibition. The greater susceptibility of *S. aureus* compared with *E. coli* is consistent with the additional outer membrane of gram-negative *E. coli*, that limits the $Zn^{2+}$/ROS release from NPs.

When applied to a fresh-cut melon and stored at 4 °C for one week, NC/ZnO films slowed microbial proliferation compared with neat NC and control melon samples. The effect of NPs morphology was evident: ZnO-SH produced the slowest increase in microbial loads, followed by ZnO-SP, whereas ZnO-FL showed the weakest inhibition among the three shapes. Under a realistic area-to-mass scenario, total Zn reached the SML at day 2 and stabilized by 7–8 mg $kg^{-1}$, with no differences among morphologies. Melons packaged with NC/ZnO-NPs films presented slightly higher pH compared with NC and melon control, consistent with antimicrobial and Zn migration results.

Current EU Regulations and EFSA guidelines were developed for plastics FCM and do not yet fully cover bio-based composites. Moreover, nanoparticle migration in FCM remains insufficiently addressed and is handled on a case-by-case basis for risk assessment. In this study, total Zn was quantified after acid digestion of the whole melon cube, so ionic and particulate forms could not be differentiated. Future work should include particle/ion discrimination using other analytical techniques for quantification, such as single particle inductively coupled plasma mass spectrometry (spICP-MS) or Asymmetric-Flow Field-Flow Fractionation (AF4). Furthermore, it would be valuable to analyse the concentration profile within the melon pulp by determining the Zn levels in direct contact with the film and in regions progressively farther from the contact surface, in order to evaluate the extent of Zn diffusion through the pulp. Additionally, the quantification of the amount of Zn remaining in the film itself after the migration step would have been of interest as a mass balance verification. Moreover, experiments were limited to one food matrix and storage condition. Evaluation of different fruits and storage conditions, combined with toxicological and sensory studies, would be relevant for better assessing consumer safety and acceptance.

Overall, NC/ZnO films, particularly those with sheet- and spherical-shaped ZnO NPs, effectively reduced microbial proliferation and maintained microbiological acceptability for at least 7 days, extending food shelf life. Achieving an appropriate balance between antimicrobial performance and zinc migration is required, give the potential toxicological implications. Overall, the effectiveness of bio-based NC/ZnO film is determined by nanomaterial choice, particle morphology, and the properties of the packaging system.

## CRediT authorship contribution statement

**Ana Rita Mendes:** Writing – original draft, Methodology, Investigation, Formal analysis. **Francisco A.G. Soares Silva:** Writing – review & editing, Methodology, Investigation. **Cristina Mena:** Writing – review & editing, Methodology. **Fátima Silva:** Writing – review & editing, Methodology. **Cristina L.M. Silva:** Writing – review & editing. **Paula Teixeira:** Writing – review & editing, Conceptualization. **Fátima Poças:** Writing – review & editing, Supervision, Resources, Conceptualization.

## Funding

This work was supported by National Funds from FCT - Fundação para a Ciência e a Tecnologia through projects UID/50016/2025 and LA/P/0076/2020 (https://doi.org/10.54499/LA/P/0076/2020) and the grant UI/BD/151387/2021 (Ana Rita Mendes).

## Declaration of competing interest

The authors declare that they have no known competing financial interests or personal relationships that could have appeared to influence the work reported in this paper.

## Appendix A. Supplementary data

Supplementary data to this article can be found online at https://doi.org/10.1016/j.foodcont.2026.112219.

## Data availability

Data will be made available on request.

## References

Abbas, M., Buntinx, M., Deferme, W., & Peeters, R. (2019). Bio)polymer/ZnO nanocomposites for packaging applications: A review of gas barrier and mechanical properties. *Nanomaterials, 9*, 1494. https://doi.org/10.3390/nano9101494

Ahmad, M. S., & Siddiqui, M. W. (2015). Factors affecting postharvest quality of fresh fruits. In M. W. Siddiqui (Ed.), *Postharvest quality assurance of fruits* (pp. 7–32). Springer International Publishing. https://doi.org/10.1007/978-3-319-21197-8_2.

Ahmadi, A., Ahmadi, P., Sani, M. A., Ehsani, A., & Ghanbarzadeh, B. (2021). Functional biocompatible nanocomposite films consisting of selenium and zinc oxide nanoparticles embedded in gelatin/cellulose nanofiber matrices. *International Journal of Biological Macromolecules, 175*, 87–97. https://doi.org/10.1016/j.ijbiomac.2021.01.135

Ahmed, M.d. W., Haque, M.d. A., Mohibbullah, M.d., Khan, M.d. S. I., Islam, M. A., Mondal, M.d. H. T., & Ahmmed, R. (2022). A review on active packaging for quality and safety of foods: Current trends, applications, prospects and challenges. *Food Packaging and Shelf Life, 33*, Article 100913. https://doi.org/10.1016/j.fpsl.2022.100913

Ansari, M. D. I., Principato, L., De Nardo, L., & Punta, C. (2026). Nanomaterials in food packaging: An overview of regulatory frameworks and migration assessment. *Food Control, 181*, Article 111707. https://doi.org/10.1016/j.foodcont.2025.111707

Babakhani, P. (2019). The impact of nanoparticle aggregation on their size exclusion during transport in porous media: One- and three-dimensional modelling investigations. *Scientific Reports, 9*, Article 14071. https://doi.org/10.1038/s41598-019-50493-6

Babayevska, N., Przysiecka, Ł., Iatsunskyi, I., Nowaczyk, G., Jarek, M., Janiszewska, E., & Jurga, S. (2022). ZnO size and shape effect on antibacterial activity and cytotoxicity profile. *Scientific Reports, 12*, 8148. https://doi.org/10.1038/s41598-022-12134-3

Basumatary, I. B., Mukherjee, A., Katiyar, V., & Kumar, S. (2022). Biopolymer-based nanocomposite films and coatings: Recent advances in shelf-life improvement of fruits and vegetables. *Critical Reviews in Food Science and Nutrition, 62*, 1912–1935. https://doi.org/10.1080/10408398.2020.1848789

Behera, S. K., Khan, G. A., Singh, S. S., Jena, B., Sashank, K., Patnaik, S., Kumar, R., Jeon, B.-H., Chakrabortty, S., Tripathy, S. K., & Mishra, A. (2024). Antibacterial efficacy of ZnO/bentonite (clay) nanocomposites against multidrug-resistant *Escherichia coli*. *ACS Omega, 9*, 2783–2794. https://doi.org/10.1021/acsomega.3c07950

Bumbudsanpharoke, N., Choi, J., Park, H. J., & Ko, S. (2019). Zinc migration and its effect on the functionality of a low density polyethylene–ZnO nanocomposite film. *Food Packaging and Shelf Life, 20*, Article 100301. https://doi.org/10.1016/j.fpsl.2019.100301

Danza, A., Conte, A., Mastromatteo, M., & Del Nobile, M. A. (2015). A new example of nanotechnology applied to minimally processed fruit: The case of fresh-cut melon. *Journal of Food Processing & Technology, 6*, Article 1000439. https://doi.org/10.4172/2157-7110.1000439

Dejene, B. K., & Abtew, M. A. (2025). Chitosan/zinc oxide (ZnO) nanocomposites: A critical review of emerging multifunctional applications in food preservation and biomedical systems. *International Journal of Biological Macromolecules, 320*, Article 144773. https://doi.org/10.1016/j.ijbiomac.2025.144773

Dejene, B. K., Birilie, A. A., Yizengaw, M. A., Getahun, S., Tadesse, T., Tsegaye, T., & Tadesse, B. (2024). Thermoplastic starch-ZnO nanocomposites: A comprehensive review of their applications in functional food packaging. *International Journal of Biological Macromolecules, 282*, Article 137099. https://doi.org/10.1016/j.ijbiomac.2024.137099

EFSA CEF Panel (EFSA Panel on Food Contact Materials, Enzymes, Flavourings and Processing Aids. (2016). Scientific opinion on the safety assessment of the substance

zinc oxide, nanoparticles, for use in food contact materials. *EFSA Journal, 14*, 4408. https://doi.org/10.2903/j.efsa.2016.4408

EFSA Scientific Committee, More, S., Bampidis, V., Benford, D., Bragard, C., Halldorsson, T., Hernandez-Jerez, A., Hougaard Bennekou, S., Koutsoumanis, K., Lambré, C., Machera, K., Naegeli, H., Nielsen, S., Schlatter, J., Schrenk, D., Silano, V., Turck, D., Younes, M., Castenmiller, J., … Schoonjans, R. (2021). Guidance on risk assessment of nanomaterials to be applied in the food and feed chain: Human and animal health. *EFSA Journal, 19*, 6768. https://doi.org/10.2903/j.efsa.2021.6768

European Commission. (2004). Regulation (EC) No 1935/2004 on food contact materials. *Official Journal of the European Union, L338*, 4–17. https://eur-lex.europa.eu/legal-content/EN/TXT/?uri=CELEX:32004R1935.

European Commission. (2005). Regulation (EC) No 2073/2005: Microbiological criteria for foodstuffs. *Official Journal of the European Union, L338*, 1–26. https://eur-lex.europa.eu/legal-content/EN/TXT/?uri=CELEX:32005R2073.

European Commission. (2011). Regulation (EU) No 10/2011 on plastic food contact materials. *Official Journal of the European Union, L12*, 1–89. https://eur-lex.europa.eu/legal-content/EN/TXT/?uri=CELEX:32011R0010.

Fadiji, T., Rashvand, M., Daramola, M. O., & Iwarere, S. A. (2023). A review on antimicrobial packaging for extending the shelf life of food. *Processes, 11*, 590. https://doi.org/10.3390/pr11020590

Fernández, A., Picouet, P., & Lloret, E. (2010). Cellulose-silver nanoparticle hybrid materials to control spoilage-related microflora in absorbent pads located in trays of fresh-cut melon. *International Journal of Food Microbiology, 142*, 222–228. https://doi.org/10.1016/j.ijfoodmicro.2010.07.001

Furlan, D. M., Morgado, D. L., Oliveira, A. J. A. de, Faceto, Â. D., Moraes, D. A. de, Varanda, L. C., & Frollini, E. (2019). Sisal cellulose and magnetite nanoparticles: Formation and properties of magnetic hybrid films. *Journal of Materials Research and Technology, 8*, 2170–2179. https://doi.org/10.1016/j.jmrt.2019.02.005

Ghule, K., Ghule, A. V., Chen, B.-J., & Ling, Y.-C. (2006). Preparation and characterization of ZnO nanoparticles coated paper and its antibacterial activity study. *Green Chemistry, 8*, 1034–1041. https://doi.org/10.1039/b605623g

Guo, Y., Yu, Z., Li, R., Wang, L., Xie, C., & Wu, Z. (2023). Cut-wounding promotes phenolic accumulation in *Cucumis melo L.* fruit (cv. Yugu) by regulating sucrose metabolism. *Horticulturae, 9*, 258. https://doi.org/10.3390/horticulturae9020258

Hakeem, M. J., Feng, J., Nilghaz, A., Ma, L., Seah, H. C., Konkel, M. E., & Lu, X. (2020). Active packaging of immobilized zinc oxide nanoparticles controls *Campylobacter jejuni* in raw chicken meat. *Applied and Environmental Microbiology, 86*. https://doi.org/10.1128/AEM.01195-20. e01195-20.

Hansini, A. M. P., Galpaya, G. D. C. P., Gunasena, M. D. K. M., Abeysundara, P. M., Kirthika, V., Bhagya, L., Gunawardana, H. D. C. N., & Koswattage, K. R. (2025). From nature to innovation: Advances in nanocellulose extraction and its multifunctional applications. *Molecules, 30*, 2670. https://doi.org/10.3390/molecules30132670

INSA (Instituto Nacional de Saúde Doutor Ricardo Jorge). (2019). *Interpretação de resultados de ensaios microbiológicos em alimentos prontos para consumo e em superfícies do ambiente de preparação e distribuição alimentar: valores-guia*. Instituto Nacional de Saúde Doutor Ricardo Jorge.

Karuppan Perumal, M. K., Rajasekaran, M. B. S., Rajan Renuka, R., Samrot, A. V., & Nagarajan, M. (2025). Zinc oxide nanoparticles and their nanocomposites as an imperative coating for smart food packaging. *Applied Food Research, 5*, Article 100849. https://doi.org/10.1016/j.afres.2025.100849

Kim, I., Viswanathan, K., Kasi, G., Thanakkasaranee, S., Sadeghi, K., & Seo, J. (2022). ZnO nanostructures in active antibacterial food packaging: Preparation methods, antimicrobial mechanisms, safety issues, future prospects, and challenges. *Food Reviews International, 38*, 537–565. https://doi.org/10.1080/87559129.2020.1737709

Kumar, L., Agwuncha, S. C., Tyagi, P., & Pal, L. (2025). Enhanced chitosan–microfibrillated cellulose hydrogen bonding for edible packaging and food shelf-life extension. *Food Packaging and Shelf Life, 52*, Article 101613. https://doi.org/10.1016/j.fpsl.2025.101613

Lebaka, V. R., Ravi, P., Reddy, M. C., Thummala, C., & Mandal, T. K. (2025). Zinc oxide nanoparticles in modern science and technology: Multifunctional roles in healthcare, environmental remediation, and industry. *Nanomaterials, 15*, 754. https://doi.org/10.3390/nano15100754

Lerch, M., Fengler, R., Mbog, G.-R., Nguyen, K. H., & Granby, K. (2023). Food simulants and real food – What do we know about the migration of PFAS from paper based food contact materials? *Food Packaging and Shelf Life, 35*, Article 100992. https://doi.org/10.1016/j.fpsl.2022.100992

Liu, L., Yuan, M., Huang, J., Geng, L., Wu, N., Yue, Y., Wang, J., & Zhang, Q. (2025). Preparation and antibacterial properties of benzisothiazolinone quaternized chitosan derivatives for sustainable fuel preservation. *Carbohydrate Polymers, 356*, Article 123379. https://doi.org/10.1016/j.carbpol.2025.123379

Maloufi, M., Djelad, A., Mokhtar, A., Reguig, K., Hasnaoui, M. A., Kebir-Medjhouda, Z. A., Ghamnia, M., & Sassi, M. (2025). Fabrication and characterization of cellulose-based packaging films with polyethylene glycol and silver nanoparticles for enhanced antimicrobial efficacy. *International Journal of Biological Macromolecules, 308*, Article 142381. https://doi.org/10.1016/j.ijbiomac.2025.142381

Mendes, A. R., Geiss, O., Bianchi, I., Ponti, J., Matos, A., Silva, C. L. M., & Poças, F. (2026). Migration of ionic and nanoparticulate zinc from nanocellulose/ZnO nanoparticles films: Morphology-dependent behaviour and modelling. *Food Additives & Contaminants: Part A*. https://doi.org/10.1080/19440049.2026.2633744. in press.

Mendes, A. R., Granadeiro, C. M., Leite, A., Geiss, O., Bianchi, I., Ponti, J., Mehn, D., Pereira, E., Teixeira, P., & Poças, F. (2025). Functional properties and safety considerations of zinc oxide nanoparticles under varying conditions. *Nanomaterials, 15*, 892. https://doi.org/10.3390/nano15120892

Mendes, A. R., Granadeiro, C. M., Leite, A., Pereira, E., Teixeira, P., & Poças, F. (2024). Optimizing antimicrobial efficacy: Investigating the impact of zinc oxide nanoparticle shape and size. *Nanomaterials, 14*, 638. https://doi.org/10.3390/nano14070638

Oms-Oliu, G., Rojas-Graü, M. A., González, L. A., Varela, P., Soliva-Fortuny, R., Hernando, M. I. H., Munuera, I. P., Fiszman, S., & Martín-Belloso, O. (2010). Recent approaches using chemical treatments to preserve quality of fresh-cut fruit: A review. *Postharvest Biology and Technology, 57*, 139–148. https://doi.org/10.1016/j.postharvbio.2010.04.001

Ortiz-Duarte, G., Pérez-Cabrera, L. E., Artés-Hernández, F., & Martínez-Hernández, G. B. (2019). Ag-chitosan nanocomposites in edible coatings affect the quality of fresh-cut melon. *Postharvest Biology and Technology, 147*, 174–184. https://doi.org/10.1016/j.postharvbio.2018.09.021

Paiva, C. A., Vilvert, J. C., Menezes, F. L. G., Leite, R. H. de L., Santos, F. K. G., Medeiros, J. F., & Aroucha, E. M. M. (2020). Extended shelf life of melons using chitosan and graphene oxide-based biodegradable bags. *Journal of Food Processing and Preservation, 44*, Article 14871. https://doi.org/10.1111/jfpp.14871

Pascall, M. A. (2020). The role and importance of packaging and labeling in assuring food safety, quality & compliance with regulations I: Packaging basics. In *Food safety and quality systems in developing countries* (pp. 261–283). Elsevier. https://doi.org/10.1016/B978-0-12-814272-1.00006-1.

Peter, A., Cozmuta, L. M., Nicula, C., Cozmuta, A. M., Apjok, R., Talasman, C. M., Drazic, G., Peñas, A., Calahorro, A. J., Kamgang Nzekoue, F., Huang, X., Sagratini, G., & Silvi, S. (2022). Barrier properties, migration into the food simulants and antimicrobial activity of paper-based materials with functionalized surface. *Polymers and Polymer Composites, 30*. https://doi.org/10.1177/09673911221106347

Poças, F., & Franz, R. (2018). Overview on European regulatory issues, legislation, and EFSA evaluations of nanomaterials. In *Nanomaterials for food packaging* (pp. 277–300). Elsevier. https://doi.org/10.1016/B978-0-323-51271-8.00010-3.

Roy, S., Kim, H. C., Panicker, P. S., Rhim, J.-W., & Kim, J. (2021). Cellulose nanofiber-based nanocomposite films reinforced with zinc oxide nanorods and grapefruit seed extract. *Nanomaterials, 11*, 877. https://doi.org/10.3390/nano11040877

Sasidharan, S., Tey, L.-H., Djearamane, S., Ab Rashid, N. K. M., Pa, R., Rajendran, V., Syed, A., Wong, L. S., Santhanakrishnan, V. K., Asirvadam, V. S., & Antony Dhanapal, A. C. T. (2024). Innovative use of chitosan/ZnO NPs bio-nanocomposites for sustainable antimicrobial food packaging of poultry meat. *Food Packaging and Shelf Life, 43*, Article 101298. https://doi.org/10.1016/j.fpsl.2024.101298

Schwan, C. L., Molitor, A., Hok, L., Ebner, P., Vipham, J. L., & Trinetta, V. (2022). Quantitative and qualitative assessments of *Enterobacteriaceae*, coliforms, and generic *Escherichia coli* on fresh vegetables sold in Cambodian fresh produce distribution centers. *Food Protection Trends, 42*, 107–112. https://doi.org/10.4315/FPT-21-023

Shahmohammadi Jebel, F., & Almasi, H. (2016). Morphological, physical, antimicrobial and release properties of ZnO nanoparticles-loaded bacterial cellulose films. *Carbohydrate Polymers, 149*, 8–19. https://doi.org/10.1016/j.carbpol.2016.04.089

Singh, S., Pereira, J., Guerreiro, P., Selbourne, C., Paula, C., Cunha, A., Sousa, C., & Poças, F. (2024). Safety profile of ZnO active packaging PBAT-based biomaterial for food packaging: First tier evaluation. *Food Control, 161*, Article 110389. https://doi.org/10.1016/j.foodcont.2024.110389

Singh, S., Şahin, G., Silva, F. A. G. S., Šinkovec, A., Grkman, J. J., Karlovits, I., & Poças, F. (2025). Development of bio-based coatings incorporating microfibrillated cellulose, lignin and ionomer dispersions for food contact applications. *Packaging Technology and Science, 38*, 613–626. https://doi.org/10.1002/pts.2906

Soares Silva, F. A. G., Bento de Carvalho, T., Dourado, F., Gama, M., Teixeira, P., & Poças, F. (2023). Performance of bacterial nanocellulose packaging film functionalised in situ with zinc oxide: Migration onto chicken skin and antimicrobial activity. *Food Packaging and Shelf Life, 39*, Article 101140. https://doi.org/10.1016/j.fpsl.2023.101140

Soares Silva, F. A. G., Dourado, F., Gama, M., & Poças, F. (2020). Nanocellulose bio-based composites for food packaging. *Nanomaterials, 10*, 2041. https://doi.org/10.3390/nano10102041

Solhi, L., Guccini, V., Heise, K., Solala, I., Niinivaara, E., Xu, W., Mihhels, K., Kröger, M., Meng, Z., Wohlert, J., Tao, H., Cranston, E. D., & Kontturi, E. (2023). Understanding nanocellulose–water interactions: Turning a detriment into an asset. *Chemical Reviews, 123*, 1925–2015. https://doi.org/10.1021/acs.chemrev.2c00611

Souza, V. G. L., Alves, M. M., Santos, C. F., Ribeiro, I. A. C., Rodrigues, C., Coelhoso, I., & Fernando, A. L. (2021). Biodegradable chitosan films with ZnO nanoparticles synthesized using food industry by-products—Production and characterization. *Coatings, 11*, 646. https://doi.org/10.3390/coatings11060646

Souza, V. G. L., Rodrigues, C., Valente, S., Pimenta, C., Pires, J. R. A., Alves, M. M., Santos, C. F., Coelhoso, I. M., & Fernando, A. L. (2020). Eco-friendly ZnO/chitosan bionanocomposites films for packaging of fresh poultry meat. *Coatings, 10*, 110. https://doi.org/10.3390/coatings10020110

Sun, J., Li, Y., Cao, X., Yao, F., Shi, L., & Liu, Y. (2022). A film of chitosan blended with ginseng residue polysaccharides as an antioxidant packaging for prolonging the shelf life of fresh-cut melon. *Coatings, 12*, 468. https://doi.org/10.3390/coatings12040468

Török, Á., Yeh, C.-H., Menozzi, D., Balogh, P., & Czine, P. (2023). European consumers' preferences for fresh fruit and vegetables – A cross-country analysis. *Journal of Agriculture and Food Research, 14*, Article 100883. https://doi.org/10.1016/j.jafr.2023.100883

Ukuku, D. O., Mukhopadhyay, S., & Olanya, M. (2018). Reducing transfer of *Salmonella* and aerobic mesophilic bacteria on melon rind surfaces to fresh juice by washing with chlorine: Effect of waiting period before refrigeration of prepared juice. *Frontiers in Sustainable Food Systems, 2*, 78. https://doi.org/10.3389/fsufs.2018.00078

Venkatesan, U., & Muniyan, R. (2024). Review on the extension of shelf life for fruits and vegetables using natural preservatives. *Food Science and Biotechnology, 33*, 2477–2496. https://doi.org/10.1007/s10068-024-01602-3

Viani, F., Rossi, B., Panzeri, W., Merlini, L., Martorana, A. M., Polissi, A., & Galante, Y. M. (2017). Synthesis and antibacterial activity of a library of 1,2-benzisothiazol-3(2H)-one (BIT) derivatives amenable to crosslinking to polysaccharides. *Tetrahedron, 73*, 1745–1761. https://doi.org/10.1016/j.tet.2017.02.025

Wu, F., Harper, B. J., & Harper, S. L. (2019). Comparative dissolution, uptake, and toxicity of zinc oxide particles in individual aquatic species and mixed populations. *Environmental Toxicology and Chemistry, 38*, 591–602. https://doi.org/10.1002/etc.4349

Youn, S.-M., & Choi, S.-J. (2022). Food additive zinc oxide nanoparticles: Dissolution, interaction, fate, cytotoxicity, and oral toxicity. *International Journal of Molecular Sciences, 23*, 6074. https://doi.org/10.3390/ijms23116074

Zhang, F., Shen, R., Li, N., Yang, X., & Lin, D. (2023). Nanocellulose: An amazing nanomaterial with diverse applications in food science. *Carbohydrate Polymers, 304*, Article 120497. https://doi.org/10.1016/j.carbpol.2022.120497